AMERICAN SOCIETY FOR MICROBIOLOGY | Infection and Immunity®

HOST RESPONSE AND INFLAMMATION

Human Three-Dimensional Endometrial Epithelial Cell Model To Study Host Interactions with Vaginal Bacteria and *Neisseria gonorrhoeae*

Paweł Łaniewski,[a] Adriana Gomez,[a] Geoffrey Hire,[a] Magdalene So,[b] Melissa M. Herbst-Kralovetz[a]

Department of Basic Medical Sciences, College of Medicine—Phoenix, University of Arizona, Phoenix, Arizona, USA[a]; Department of Immunobiology and BIO5 Institute, College of Medicine—Tucson, University of Arizona, Tucson, Arizona, USA[b]

ABSTRACT Colonization of the endometrium by pathogenic bacteria ascending from the lower female reproductive tract (FRT) is associated with many gynecologic and obstetric health complications. To study these host-microbe interactions *in vitro*, we developed a human three-dimensional (3-D) endometrial epithelial cell (EEC) model using the HEC-1A cell line and the rotating wall vessel (RWV) bioreactor technology. Our model, composed of 3-D EEC aggregates, recapitulates several functional/structural characteristics of human endometrial epithelial tissue, including cell differentiation, the presence of junctional complexes/desmosomes and microvilli, and the production of membrane-associated mucins and Toll-like receptors (TLRs). TLR function was evaluated by exposing the EEC aggregates to viral and bacterial products. Treatment with poly(I·C) and flagellin but not with synthetic lipoprotein (fibroblast-stimulating lipoprotein 1 [FSL-1]) or lipopolysaccharide (LPS) significantly induced proinflammatory mediators in a dose-dependent manner. To simulate ascending infection, we infected EEC aggregates with commensal and pathogenic bacteria: *Lactobacillus crispatus*, *Gardnerella vaginalis*, and *Neisseria gonorrhoeae*. All vaginal microbiota and *N. gonorrhoeae* efficiently colonized the 3-D surface, localizing to crevices of the EEC model and interacting with multiple adjacent cells simultaneously. However, only infection with pathogenic *N. gonorrhoeae* and not infection with the other bacteria tested significantly induced proinflammatory mediators and significant ultrastructural changes to the host cells. The latter observation is consistent with clinical findings and illustrated the functional specificity of our system. Additionally, we highlighted the utility of the 3-D EEC model for the study of the pathogenesis of *N. gonorrhoeae* using a well-characterized Δ*pilT* mutant. Overall, this study demonstrates that the human 3-D EEC model is a robust tool for studying host-microbe interactions and bacterial pathogenesis in the upper FRT.

KEYWORDS female reproductive tract, *Gardnerella vaginalis*, innate immunity, *Lactobacillus*, membrane-associated mucin, *Neisseria gonorrhoeae*, organotypic model, rotating wall vessel bioreactor, uterine, Toll-like receptor

Human upper female reproductive tract (FRT) infections are presumed to result from pathogenic bacteria ascending from the lower FRT. Colonization of the endometrium by these microbes is associated with complications of gynecologic and reproductive health, including endometritis, pelvic inflammatory disease (PID) (1, 2), preterm delivery, and spontaneous abortions (3), resulting in a significant public health impact. Historically, the endometrium of healthy women has been considered to be a sterile environment. However, the use of next-generation sequencing techniques has en-

Received 22 December 2016 **Accepted** 23 December 2016

Accepted manuscript posted online 4 January 2017

Citation Łaniewski P, Gomez A, Hire G, So M, Herbst-Kralovetz MM. 2017. Human three-dimensional endometrial epithelial cell model to study host interactions with vaginal bacteria and *Neisseria gonorrhoeae*. Infect Immun 85:e01049-16. https://doi.org/10.1128/IAI.01049-16.

Editor Andreas J. Bäumler, University of California, Davis

Address correspondence to Melissa M. Herbst-Kralovetz, mherbst1@email.arizona.edu.

hanced our understanding of the complexity and number of microbiota that inhabit human mucosal surfaces. Recent reports showed that the sites of the body that were previously thought to be devoid of bacteria, such as the lung (4), bladder (5, 6), placenta (7), as well as the endometrium (8, 9), harbor unique, low-abundance microbiota.

Cervical mucus contains a high concentration of cytokines (10), antimicrobial peptides (11), and immunoglobulins and matrix metalloproteinases (12) that function to protect the uterus against bacterial colonization. However, many studies indicate that bacteria from the lower FRT are nevertheless able to cross these physical and physiological barriers. For example, Hansen et al. showed that the cervical mucus plug only inhibits and does not block the passage of *Ureaplasma parvum* during its ascension from the vagina through the cervical canal (13).

Bacterial vaginosis (BV) is the most common vaginal disorder worldwide and is characterized as a depletion of commensal lactobacilli and the overgrowth of *Gardnerella vaginalis* and other anaerobic and microaerophilic bacteria (14). The role of *G. vaginalis* in BV is still controversial. Schwebke and colleagues hypothesize that *G. vaginalis* is sexually transmitted and initiates polymicrobial biofilm formation (15, 16). Importantly, BV has a high recurrence rate and is difficult to treat (17). Furthermore, BV is associated with serious reproductive sequelae, including endometritis and PID (1, 2).

Mitchell et al. tested for the presence of vaginal bacterial species, including commensal lactobacilli (i.e., *Lactobacillus crispatus*, *Lactobacillus iners*, and *Lactobacillus jensenii*) and BV-associated bacteria (*Gardnerella vaginalis*, *Atopobium vaginae*, *Megasphaera* spp., *Prevotella* spp., *Leptotrichia/Sneathia* spp., BVAB1, BVAB2, and BVAB3), in endometrial samples collected from patients undergoing hysterectomy using quantitative PCR assays (18). The study revealed that uteri from 90% of enrolled patients were colonized with at least one vaginal species. Another study tested for the presence of BV-associated bacteria in endometrial specimens using fluorescence *in situ* hybridization (FISH) (19) and found that 50% of pregnant and nonpregnant women with BV had an endometrium covered with a *G. vaginalis*-dominated polymicrobial biofilm.

Chlamydia trachomatis and *Neisseria gonorrhoeae* are common etiological agents of sexually transmitted infections (STI) and are associated with chronic endometritis (20). The Centers for Disease Control and Prevention guidelines include gonococcal endometritis, which is well-characterized syndrome, as a manifestation of PID (http://www.cdc.gov/std/tg2015/pid.htm). Wiesenfeld et al. confirmed the association of gonococcal infection with PID by detecting subclinical PID in 26% of women with cervical gonococcal infections but only 11% of women without gonorrhea. Coinfection with *N. gonorrhoeae* and *C. trachomatis* increased the rate of subclinical PID to 39%, whereas the rate of subclinical PID was 9% for women not infected (21).

To study host-microbe interactions in the endometrium, we developed and characterized a three-dimensional (3-D) human endometrial epithelial cell (EEC) culture model, using the rotating wall vessel (RWV) bioreactor technology. Previous 3-D cell culture models have been shown to faithfully recapitulate many morphological and physiological characteristics of tissue *in vivo*. These cultures not only preserve the cellular architecture of this tissue but also respond to external stimuli in ways that mimic the response in the *in vivo* microenvironment (22–27). To our knowledge, this is the first report describing a bioreactor-derived 3-D EEC culture model. In this study, we characterized the morphology and structure of the 3-D EEC model as well as the innate immune responses after microbial challenge. For infection studies, we used a reductionist approach and utilized three species individually, each of which has been shown to ascend from the lower FRT (vagina and cervix) to the upper FRT (uterus): *L. crispatus*, a commensal species associated with vaginal health; *G. vaginalis*, a predominant species in BV; and *N. gonorrhoeae*, the species responsible for sexually transmitted gonorrhea. Our results demonstrate that all vaginal bacterial species and *N. gonorrhoeae* efficiently colonize the 3-D EEC aggregates. We observed that gonococci induce dramatic morphological changes to the cortex of epithelial cells. Additionally, this is the first report showing that bacterial colonies interact with multiple adjacent 3-D cuboidal cells, mostly at their crevices and folds. These phenomena could not be detected in

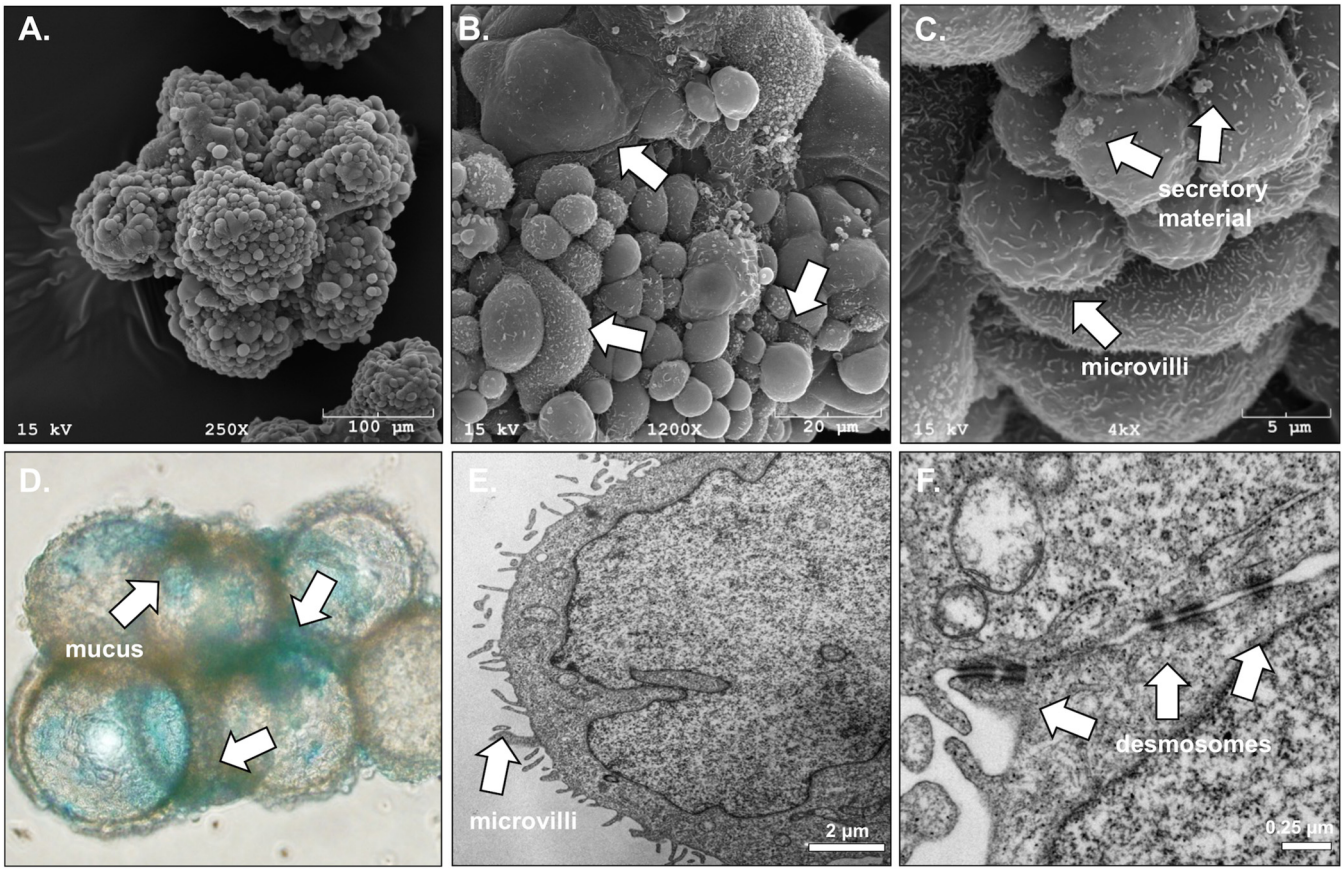

FIG 1 Structural characteristics of cells in the human 3-D endometrial epithelial cell model. (A to C) An EEC aggregate at day 21 visualized by SEM at magnifications of ×250, ×1,200, and ×4,000, respectively; (D) light microscopy following alcian blue staining at a magnification of ×20; (E, F) TEM. (A) A fully developed EEC aggregate after 21 days of growth; the carrier beads are covered with a single layer of endometrial epithelial cells. (B) White arrows indicate cells at different stages of proliferation and differentiation, especially with reference to the number of microvilli present on the cell surface. On the other panels, white arrows indicate microvilli (A, C), mucus/secretory material (A, B), and junctional complexes (i.e., desmosomes) (D).

traditional monolayer cultures. We also observed that the 3-D EEC model produced significant levels of proinflammatory immune mediators following infection with pathogenic gonococci but not following infection with the other tested vaginal bacteria. Moreover, using a well-characterized *N. gonorrhoeae* Δ*pilT* mutant, which produces nonretractible pilus fibers, we showed that host-microbe interaction is strain dependent. Overall, the studies highlighted in this report demonstrate that the human 3-D EEC model is a robust tool to study the host innate immune responses to microbial challenges in the upper FRT.

RESULTS

Morphological characteristics of the human 3-D EEC model. To construct the human 3-D endometrial epithelial cell (EEC) model, we used the rotating wall vessel (RWV) bioreactor technology (28) and the previously established endometrial epithelial cell line HEC-1A. The HEC-1A cell line was isolated in 1968 by H. Kuramoto from a patient with stage IA endometrial cancer (29). These cells were initially grown as monolayers in a tissue culture flask and then transferred to an RWV bioreactor along with collagen-coated porous microcarrier beads. The rotation of the bioreactor creates a low-fluid-shear microgravity environment that maintains the cells in free fall. In this environment, cells utilize the beads as a growth scaffold and form 3-D cellular aggregates. The progression of aggregate formation was periodically monitored by bright-field light and electron microscopy. The formation of aggregates, consisting of microcarrier beads completely covered with endometrial epithelial cells, occurred by day 21 in culture (Fig. 1A). Transmission electron microscopy (TEM) and scanning electron

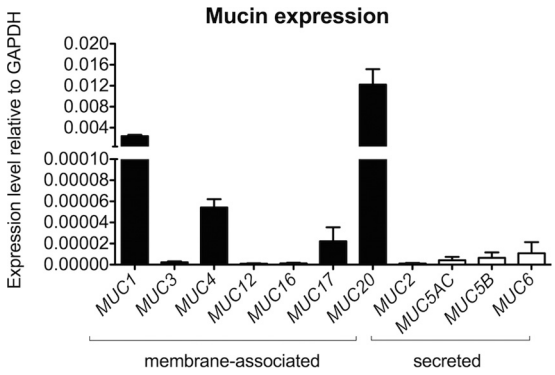

FIG 2 Cells in the human 3-D endometrial epithelial cell model express membrane-associated mucins (MUC1, MUC4, MUC17, and MUC20). The EEC aggregates were profiled for mucin expression by qRT-PCR analysis using total RNA from lysed cells. The expression of each gene was normalized to the level of expression of the *GAPDH* gene using the $2^{-\Delta CT}$ method. The results shown are means ± SD values from five independent experiments, each of which was performed in duplicate.

microscopy (SEM) images of these bioreactor-generated human EEC aggregates showed several hallmarks of cellular differentiation and polarization (Fig. 1). First, SEM examination revealed that HEC-1A cells in 3-D culture adhered to collagen-coated beads and grew as a single layer (Fig. 1A), whereas in our experience, other cancer cell lines do not attach to the collagen-coated beads but, rather, form aggregates independently of the beads. Furthermore, the observed morphology of the cells from the bioreactor-derived aggregates was similar to the morphology of nonciliated cells from human endometrial tissue in the early proliferative phase of the menstrual cycle, as evidenced by SEM. The cells had a convex apical shape, were nonciliated, and had various levels of microvilli ranging from dense to sparse coverage. In addition, secretory material and deposits were observed between adjacent cells and on the apical cell surface. These ultrastructural features of this simple cuboidal layer of epithelium are consistent with and have a remarkable similarity with those seen in previous SEM images of the human endometrium (30), particularly in the 3-D appearance of the epithelial cells not observed in monolayers (Fig. 1B). Subsequent evaluation of the aggregates by SEM and TEM showed that endometrial epithelial cells grown in 3-D aggregates develop ultrastructures, including microvilli (Fig. 1C and E) and junctional complexes/desmosomes (Fig. 1F), and produce mucus/secretory material (Fig. 1C and D). These features recapitulate the morphological characteristics of the tissue *in vivo*, suggesting that the 3-D culture system allows a high degree of cell differentiation toward an endometrial cell phenotype.

Cells in the human 3-D endometrial epithelial cell model express membrane-associated mucins. SEM images revealed the presence of secreted globular material on the surface of 3-D EEC aggregates (Fig. 1C). Using the cationic dye alcian blue, which selectively stains acidic mucins, a major component of mucus, we confirmed that these secretions contained mucus. Stained 3-D aggregates were visualized by bright-field light microscopy (Fig. 1D). To further identify the types of mucins being expressed by the human 3-D EEC aggregates, we performed quantitative reverse transcription-PCR (qRT-PCR) using primers directed against gene transcripts of the membrane-associated mucins (MAMs) *MUC1*, *MUC3*, *MUC4*, *MUC12*, *MUC16*, *MUC17*, and *MUC20*, as well as against transcripts of the secreted gel-forming mucins *MUC2*, *MUC5AC*, *MUC5B*, and *MUC6*. We observed that two MAMs, *MUC1* and *MUC20*, are expressed at the highest levels, 0.002 and 0.012, respectively, compared to the level of expression of the internal standard, the gene for glyceraldehyde-3-phosphate dehydrogenase (*GAPDH*) (Fig. 2). *MUC4* and *MUC17* gene transcripts were expressed at lower magnitudes (0.00005 and 0.00002, respectively, compared to the level of expression of the *GAPDH* gene transcript). We also observed very low levels of expression of secreted gel-forming mucins *MUC5AC*, *MUC5B*, and *MUC6* in our model. Other tested mucins, namely, *MUC2*, *MUC3*,

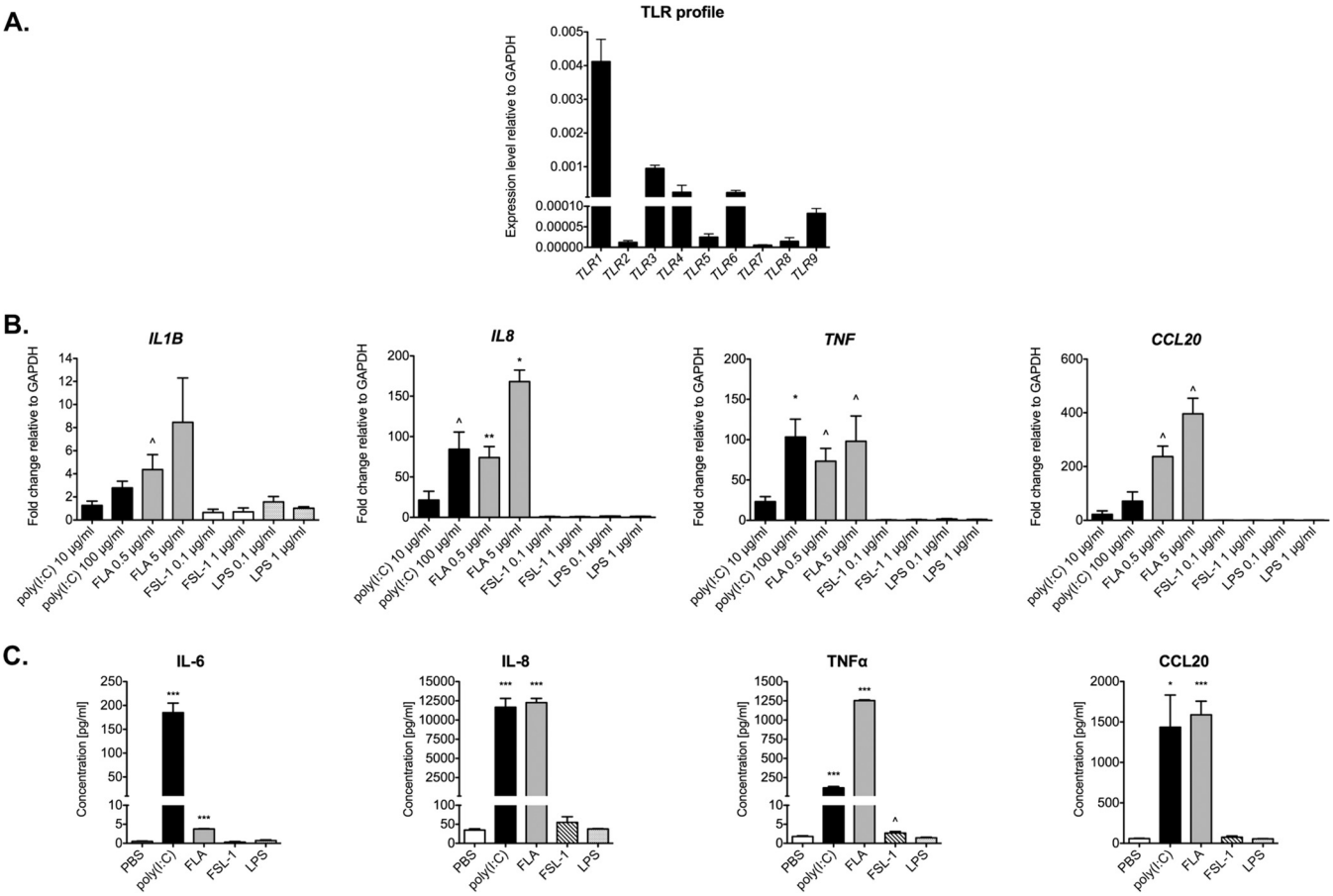

FIG 3 Innate immune response of cells in the human 3-D endometrial epithelial cell model following microbial product exposure. (A) Expression profile of TLR1 to TLR9. EEC aggregates were profiled for TLR1 to TLR9 by qRT-PCR analysis using total RNA from lysed cells. The level of expression of each gene was normalized to the level of expression of the *GAPDH* gene using the $2^{-\Delta CT}$ method. The results shown are means ± SD values from three independent experiments, each of which was performed in duplicate. (B, C) Increased levels of proinflammatory cytokines and chemokines following exposure to microbial products. EEC aggregates were exposed to the indicated concentrations of the following microbial products for 24 h: poly(I·C), flagellin (FLA), fibroblast-stimulating lipoprotein 1 (FSL-1), and lipopolysaccharide (LPS). (B) The levels of expression of the *IL-1B*, *IL-8*, *TNF*, and *CCL20* transcripts were determined by qRT-PCR analysis using total RNA from lysed cells. mRNA levels were first normalized to the level of the *GAPDH* gene and then compared to those for PBS-treated samples, and the fold change was calculated using the $2^{-\Delta\Delta CT}$ method. (C) The levels of IL-6, IL-8, TNF-α, and CCL20 secreted in supernatants from the cell cultures treated with the highest dose of TLR agonists were measured by use of a BioPlex array. Data are shown as means ± SDs from three independent experiments, each of which was performed in duplicate. *P* values were calculated by an unpaired two-tailed Student *t* test. ^, $P < 0.05$; *, $P < 0.01$; **, $P < 0.001$; ***, $P < 0.0001$.

MUC12, and *MUC16*, were minimally expressed. Nevertheless, these data demonstrate that MAMs are expressed in the human endometrial cells in the 3-D cell culture.

Cells in the human 3-D endometrial epithelial cell model produce proinflammatory cytokines and chemokines following exposure to microbial products. The innate immune response is considered the first line of defense against microbial pathogens. TLRs play a crucial role in this response by recognizing a broad range of microbial products. To profile TLR expression in the human 3-D endometrial epithelial cell model, we performed qRT-PCR targeting the *TLR1* to *TLR9* genes. TLR gene expression was positive for all tested TLRs (Fig. 3A). All amplified products were at the predicted size for their respective mRNAs (data not shown). In particular, our human 3-D EEC aggregates expressed *TLR1*, *TLR3*, and *TLR6* at a relatively high level compared to the level of expression of the *GAPDH* gene, while the levels of expression of *TLR2* and *TLR7* were comparatively low. Importantly, this TLR expression profile was consistent with the TLR expression profile in primary endometrial tissue (31) and in primary human endometrial epithelial cells (32) reported by others.

To study the functionality of TLRs in our model, we treated 3-D EEC aggregates with selected microbial products for 24 h, after which expression of proinflammatory

cytokine and chemokine mRNAs was quantified by qRT-PCR. We chose one viral product, poly(I·C), which is a known TLR3 agonist, and three bacterial products (flagellin, fibroblast-stimulating lipoprotein 1 [FSL-1], and lipopolysaccharide [LPS]), which are recognized by TLR5, TLR2/6, and TLR4, respectively. Treatment with either poly(I·C) or flagellin increased the expression level of all tested cytokines and chemokines, i.e., interleukin-1β (IL-1β), interleukin-8 (IL-8), tumor necrosis factor alpha (TNF-α), and chemokine (C-C motif) ligand 20 (CCL20) (Fig. 3B). IL-1β expression was increased by 2.8-fold after poly(I·C) treatment (100 μg/ml) ($P < 0.05$) relative to that for the phosphate-buffered saline (PBS)-treated controls. Flagellin at 0.5 and 5 μg/ml also induced the level of IL-1β expression (by 4.4- and 8.5-fold, respectively); however, these changes were not statistically significant compared to the results for the PBS-treated controls. The IL-8 expression level increased significantly following treatment with 100 μg/ml poly(I·C) (84.3-fold; $P < 0.05$) and 0.5 μg/ml and 5 μg/ml flagellin (74.0-fold [$P < 0.001$] and 168.0-fold [$P < 0.01$], respectively) relative to that for the PBS-treated controls. Similarly, TNF-α mRNA levels were significantly higher in human endometrial cells in the 3-D cell culture treated with either dose of poly(I·C) (23.1-fold for 10 μg/ml [$P < 0.05$] and 103.3-fold for 100 μg/ml [$P < 0.01$]) and flagellin (73.3-fold for 0.5 μg/ml [$P < 0.05$] and 97.9-fold for 5 μg/ml [$P < 0.05$]). CCL20 expression levels also increased following exposure to flagellin (237.1-fold for 0.5 μg/ml [$P < 0.05$] and 396.2 for 5 μg/ml [$P < 0.05$]). We observed a 71.1-fold increase in the level of CCL20 expression after poly(I·C) treatment (100 μg/ml); however, it was not statistically significant. In contrast to our results with poly(I·C) and flagellin, exposure of human endometrial cells in the 3-D cell culture to FSL-1 (a synthetic bacterial lipoprotein) or LPS did not result in any detectable increase in the level of expression of any of the proinflammatory cytokines or chemokines tested (Fig. 3B).

To confirm these results, we also assayed cell supernatants using multiplex cytometric bead arrays to quantify the levels of secreted proinflammatory cytokines and chemokines. Patterns of cytokine and chemokine secretion mirrored the data generated by qRT-PCR (Fig. 3C). To summarize, we have shown that poly(I·C) (a viral product) and flagellin (a bacterial product) but not FSL-1 or LPS are able to significantly induce the expression of proinflammatory cytokines and chemokines in the 3-D human EEC model in a dose-dependent manner.

Vaginal bacterial species and *N. gonorrhoeae* colonize cells in the human 3-D endometrial epithelial cell model. Previous reports have shown that vaginal microbiota are able to ascend to the upper FRT and invade the endometrium (18, 19, 33). To study host-microbe interactions in our human 3-D EEC model, we infected EEC aggregates with commensal and pathogenic vaginal bacteria, namely, *L. crispatus* strain VPI-3199, *G. vaginalis* strain JCP8066, *Mobiluncus mulieris* strain UPII 28-I, or *N. gonorrhoeae* MS11. For vaginal bacteria, we exposed the cells at a supraphysiological multiplicity of infection (MOI) of 100 for the purpose of electron microscopy. At 24 h postinfection, we used scanning electron microscopy to determine colonization through direct visualization of bacterial adherence to the 3-D EEC surface (Fig. 4). We observed that all tested bacterial species were able to adhere to the surfaces of cells in the EEC aggregates. Indeed, *L. crispatus* and *G. vaginalis* were able to form clusters of bacterial cells attached to the surface of the aggregates, as seen on SEM images (Fig. 4A and B). These observed interactions between bacterial cells on the aggregate surface could reflect an early stage of biofilm formation.

N. gonorrhoeae adhered to the surfaces of cells in the 3-D EEC aggregates as microcolonies. The microcolonies were often located at the crevices and folds between adjacent cells, and individual microcolonies interacted with the adjacent EECs. Microvilli beneath and close to the bacteria were elongated, and the microcolonies often interacted with multiple cells simultaneously. *N. gonorrhoeae* is known to form microcolonies and induce the elongation of microvilli during infection of monolayer epithelial cells. The phenotype in the EEC model mirrors these established phenotypes. The 3-D nature of the EEC model revealed phenotypes that could not be detected in monolayer epithelial cells, i.e., the location of microcolonies in the crevices and folds of

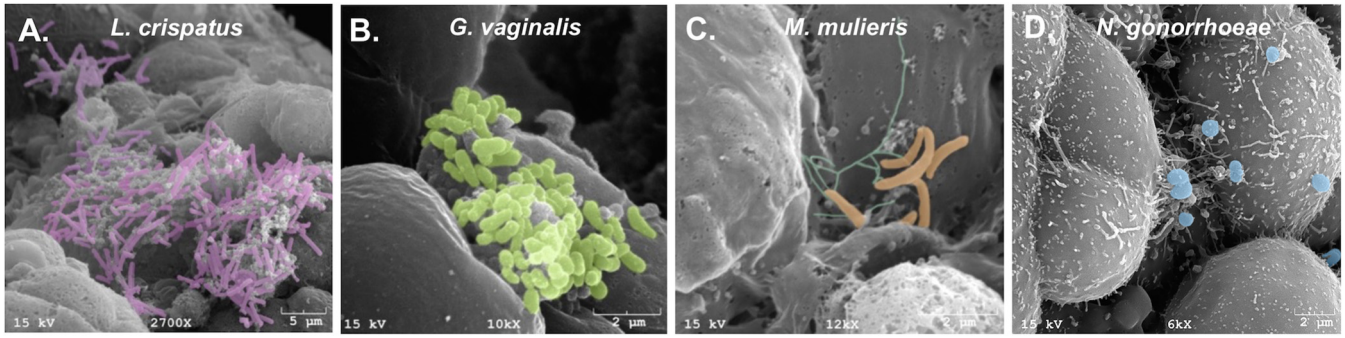

FIG 4 Vaginal bacterial species and *N. gonorrhoeae* effectively colonize cells in the human 3-D endometrial epithelial cell model. Scanning electron micrographs of EEC aggregates infected with *L. crispatus* VPI-3199 (A), *G. vaginalis* JCP8066 (B), *M. mulieris* UPII 28-I (C), and *N. gonorrhoeae* MS11 (D) for 24 h are shown. SEM images show the characteristic morphologies of each species attached to the surface of EEC aggregates. (A to D) Bacterial colonies interact with several cells simultaneously and localize to folds and crevices of the 3-D EEC model. Bacteria were pseudocolored using Photoshop CS5.1 software (Adobe, San Jose, CA): purple for *L. crispatus* bacilli (A), green for *G. vaginalis* coccobacilli (B), orange for the curved rods of *M. mulieris* and turquoise for putative pili of *M. mulieris* (C), and blue for *N. gonorrhoeae* diplococci (D).

cells and the interaction of microcolonies with multiple cells. Overall, these data illustrate that selected bacterial species that reside in the lower FRT can adhere to cells in the human 3-D EEC model, suggesting that our 3-D model could be used to study host-microbe interactions and, potentially, the steps in biofilm formation.

Cells in the human 3-D endometrial epithelial cell model produce proinflammatory cytokines and chemokines following infection with pathogenic gonococci but not following infection with vaginal bacterial species. To study the host immune response following bacterial colonization, we infected human 3-D EEC aggregates with individual species of commensal and pathogenic bacteria that reside in the human FRT. The following species were selected for study: *L. crispatus* (strain VPI-3199), which is a commensal in the vaginal microbiota and is associated with vaginal health; *G. vaginalis*, two strains of which, namely, JCP8066, isolated from an asymptomatic (BV-negative) woman, and JCP8151B, isolated from a symptomatic (BV-positive) woman were studied; and *N. gonorrhoeae*, consisting of strain MS11 of this sexually transmitted pathogen. Human 3-D EEC aggregates were infected with each bacterial strain at an MOI of 10 for 24 h, followed by RNA isolation and quantification of mRNA transcripts encoding proinflammatory cytokines (IL-1β, IL-8, and TNF-α) and the chemokine CCL20 by qRT-PCR. We confirmed the colonization of 3-D EEC aggregates by a plating assay (see Materials and Methods). We also measured cytotoxicity in 3-D EEC aggregates following bacterial infections at an MOI of 10 using a lactate dehydrogenase (LDH) cytotoxicity assay. We observed low levels of cytotoxicity ($<$5%) following infection (data not shown).

Our results demonstrated that infection with *N. gonorrhoeae* upregulated the expression of all three cytokines and as well as the CCL20 chemokine (Fig. 5). Following gonococcal infection, the level of expression of IL-1β transcripts increased by 2.4-fold compared to that for the PBS-treated control, although this difference was not statistically significant. IL-8 and TNF-α mRNA levels were significantly induced (77-fold and 29.6-fold, respectively; $P < 0.05$), and the level of CCL20 mRNA expression was also robustly induced by 90.6-fold ($P < 0.05$). In contrast to the results obtained with *N. gonorrhoeae*, neither the commensal *L. crispatus* strain nor the BV-associated *G. vaginalis* strain elicited any significant increases in the levels of mRNA for the tested proinflammatory mediators compared to those for the PBS-treated negative-control group (Fig. 5A). Additionally, we infected 3-D EEC aggregates with lower doses of *N. gonorrhoeae* MS11 (i.e., at MOIs of 1 and 5) as well as heat-inactivated bacteria. The expression levels of the *IL-8*, *TNF*, and *CCL20* transcripts were dose dependent after the gonococcal infection. Moreover, heat-inactivated *N. gonorrhoeae* did not induce the expression of the tested cytokines/chemokines, which indicates that live bacteria are required to induce the host immune response (Fig. 5A). To confirm these results on

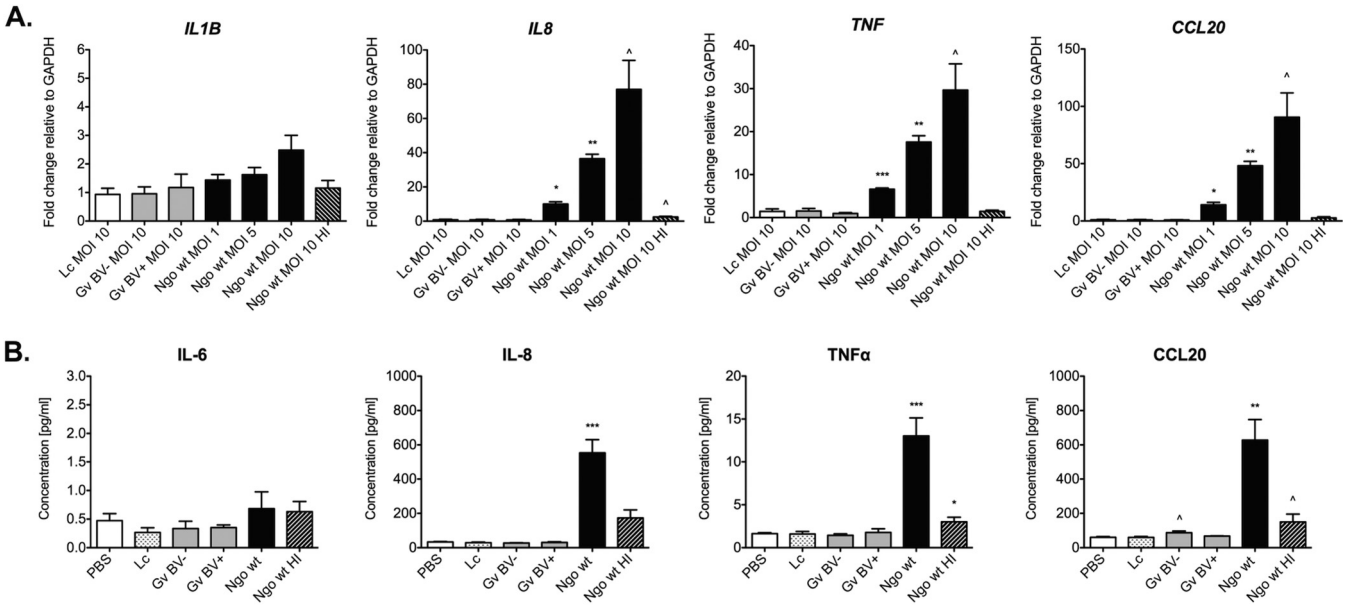

FIG 5 Increased levels of proinflammatory cytokines and chemokines following infection with *N. gonorrhoeae* but not with *L. crispatus* or *G. vaginalis*. Human EEC aggregates were infected with *L. crispatus* VPI-3199, *G. vaginalis* JCP8066 from a BV-negative woman, *G. vaginalis* JCP8151B from a BV-positive woman, or *N. gonorrhoeae* MS11 at the indicated MOIs. *N. gonorrhoeae* was heat inactivated (HI) at 55°C for 30 min. (A) The levels of expression of the *IL-1B*, *IL-8*, *TNF*, and *CCL20* transcripts were determined by qRT-PCR using total RNA from lysed cells. mRNA levels were first normalized to the level of mRNA for the GAPDH gene and then compared to those for PBS-treated samples, and the fold change was calculated using the $2^{-\Delta\Delta CT}$ method. (B) The levels of secreted IL-6, IL-8, TNF-α, and CCL20 in supernatants from the cell cultures infected at an MOI of 10 were measured by use of a BioPlex array. Data are shown as the means ± SDs from at least three independent experiments, each of which was performed in duplicate. Lc, *L. crispatus* VPI-3199; Gv BV−, *G. vaginalis* JCP8066 from a BV-negative woman; Gv BV+, *G. vaginalis* JCP8151B from a BV-positive woman; Ngo, *N. gonorrhoeae* MS11; wt, wild type. *P* values were calculated by an unpaired two-tailed Student *t* test. ^, $P < 0.05$; *, $P < 0.01$; **, $P < 0.001$; ***, $P < 0.0001$.

the protein level, we also assayed cell supernatants using multiplex cytometric bead arrays to quantify the levels of secreted proinflammatory cytokines and chemokines. Only live *N. gonorrhoeae* MS11 induced the secretion of IL-8, TNF-α, and CCL20 ($P < 0.001$) (Fig. 5B).

The *N. gonorrhoeae* wt and Δ*pilT* mutant interact with cells in the human 3-D endometrial epithelial cell model in a strain-dependent manner. To show the utility of our model to study *N. gonorrhoeae* pathogenesis, we infected 3-D EEC aggregates with wild-type (wt) strain *N. gonorrhoeae* MS11 and its isogenic Δ*pilT* mutant. The *pilT* gene encodes an ATPase which is required for retraction of type 4 pilus (Tfp) fibers. This retraction process is known to induce changes in the infected epithelial cell at many levels, including the elongation of microvilli beneath and in proximity to attached gonococci. SEM analysis of 3-D EEC aggregates infected at an MOI of 10 for 24 h showed that both strains adhered to 3-D EEC aggregates. The wild-type strain induced dramatic remodeling of the microvillus architecture. Microvilli underneath and in proximity to bacteria appeared stretched and elongated (Fig. 6B). This event was not observed in EECs infected with the Δ*pilT* mutant (Fig. 6F). EECs infected with wild-type bacteria appeared healthy, while EECs infected with the Δ*pilT* mutant lost their structural integrity (Fig. 6C, D, G, and H). It has been shown with monolayer epithelial cells that Δ*pilT* mutant-infected cells undergo apoptosis (34). The loss of cellular integrity observed here is consistent with the findings of these studies.

Finally, qRT-PCR analysis of EECs in the 3-D cell culture infected with the *N. gonorrhoeae* wild type and the Δ*pilT* mutant showed that pilus retraction also influenced the expression of *IL-8* and *NFKB1*. The wt strain induced significantly higher levels of mRNA for the proinflammatory chemokine IL-8 (1.6-fold, $P < 0.0001$) as well as the levels of mRNA for the NF-κB p105 subunit (2.3-fold, $P < 0.0001$) than the Δ*pilT* mutant.

DISCUSSION

The RWV bioreactor technology has previously been utilized to create organotypic models of a variety of mucosal sites, including endocervical and vaginal tissues (23, 24,

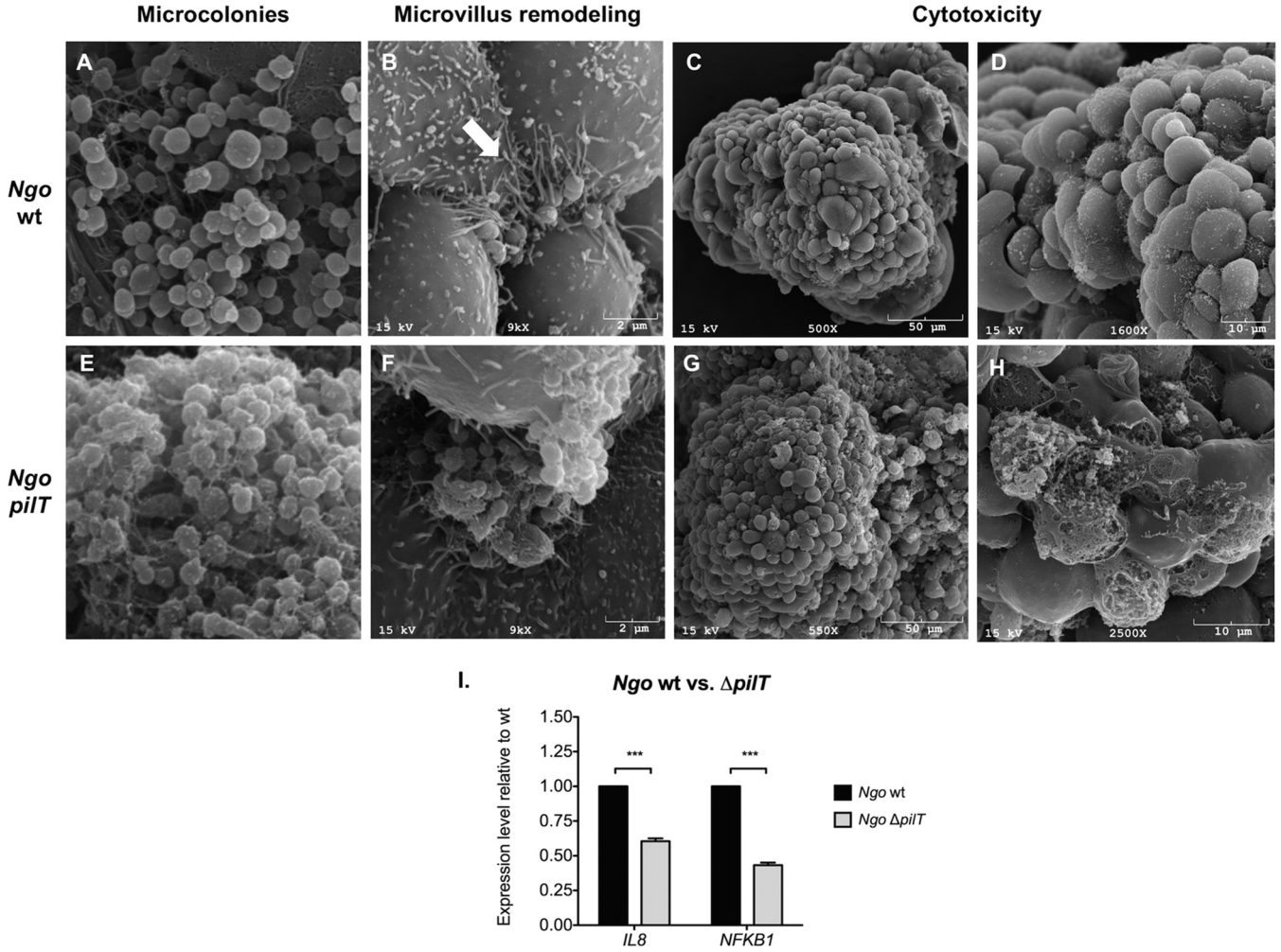

FIG 6 The *N. gonorrhoeae* Δ*pilT* mutant does not rearrange the microvillus architecture of 3-D EEC aggregates like the wild type does and exhibits a higher level of cytotoxicity and induces lower levels of IL-8 than the wild type. (A, E) Scanning electron micrographs of EEC aggregates infected with the *N. gonorrhoeae* MS11 wt (A) and the Δ*pilT* mutant (E) at an MOI of 10 for 24 h. (B, F) A microcolony of wt *N. gonorrhoeae* but not a microcolony of the Δ*pilT* mutant induces microvillus remodeling. Arrow, stretched and elongated microvilli after infection with the wt. Some microvillus distal ends appear to adhere to individual gonococci. Microcolonies localize to the folds and crevices of the 3-D EEC aggregates and interact with multiple adjacent cells simultaneously. (C, D, G, H) The Δ*pilT* mutant induces a greater cytotoxic effect on 3-D EEC aggregates than the wt. Images at two different magnifications were used to highlight destroyed EECs in the 3-D cell culture after Δ*pilT* infection. (I) Δ*pilT* induces lower levels of *IL-8* and *NFKB1* than the wt. Expression levels were determined by qRT-PCR using total RNA from lysed cells. mRNA levels were first normalized to the *GAPDH* mRNA level and then compared to those for samples infected with the wt. The fold change was calculated using the $2^{-\Delta\Delta CT}$ method.

35, 36). Previous studies aimed at modeling the endometrium have utilized tissue explants, in which tissue integrity is preserved, but an intact architecture is maintained only for a relatively short time *in vitro* and is limited by the availability of fresh tissue (37–39). Other approaches to 3-D EEC cultures have included an organotypic model in which epithelial cells isolated from the endometrium are cultivated as glandular organoids within a Matrigel matrix or fibrin-agarose scaffolds in coculture with stromal cells seeded on plastic (40, 69). A future enhancement of our 3-D EEC model could be coculturing of HEC-1A cells with stromal cells. Currently, we demonstrate that the RWV bioreactor-derived 3-D EEC model can serve as a valuable tool to study host-microbe interactions at this mucosal site.

HEC-1A cells (ATTC HTB-112) were selected to generate our 3-D endometrial model based on available EEC lines. This cell line was isolated in 1968 from a woman with endometrial adenocarcinoma (29) and has been used widely to study the molecular mechanisms underlying the physiology and pathology of the human FRT. One might argue that a 3-D model generated from a cell line that was immortalized from primary

human tissue would recapitulate *in vivo* characteristics even more accurately. However, all endometrial epithelial cell lines currently available from ATCC (i.e., the AN3 CA, HEC-1A, HEC-1B, KLE, and RL59-2 cell lines) are of tumor origin. Two other immortalized normal epithelial cell lines, human endometrial surface epithelial cells (HES) and human telomerase reverse transcriptase-immortalized EECs, were recently shown to be HeLa cervical carcinoma and MCF-7 breast cancer cells, respectively (41). The latter study also demonstrated that the HEC-1A cell line is uncontaminated (as determined by short tandem repeat profiling) and is predominantly diploid, unlike other lines, such as the HEC-1B cell line, which is tetraploid (41).

The endometrial epithelium is the first uterine cell layer that encounters microbes ascending from the lower FRT. To demonstrate that our model is a suitable tool for investigating innate immune mechanisms in the human endometrium, we validated the expression of TLRs in the 3-D EEC model. Previous reports had shown the presence of TLR1 to TLR6 (42) and TLR7 to TLR10 (31) by immunostaining of formalin-fixed human primary endometrial tissues from biopsy specimens, with the latter study also reporting qRT-PCR data for TLR7 to TLR10. In a third study, Schaefer and colleagues (32) demonstrated that cultures of human EEC-1 cells express TLR1 to TLR9 but not TLR10, as measured by qRT-PCR. Our results from HEC-1A cells grown in 3-D cell culture are in agreement with those of all three studies of biopsy specimens or primary endometrial epithelium demonstrating expression of all tested TLRs (TLR1 to TLR9) (Fig. 3A), with the level of expression of TLR7 being the lowest (32).

Beyond monitoring their expression, we also determined the ability of the TLRs expressed in our 3-D EEC aggregates to respond to their cognate agonists. We demonstrated that stimulation with both a viral product [poly(I·C)] and a bacterial product (flagellin), which are recognized by TLR3 and TLR5, respectively, activates a proinflammatory cytokine response (Fig. 3B), likely through activation of NF-κB and mitogen-activated protein kinase pathways. In contrast, treatment with FSL-1 (a synthetic lipoprotein that is a TLR2/6 agonist) or LPS (a TLR4 agonist) did not result in the expression of proinflammatory mediators, despite the expression of TLR2, TLR4, and TLR6; however, this observation is in agreement with a previous report also showing a lack of response by HEC-1A cells to the FSL-1 ligand (43). One possible explanation could be that HEC-1A cells do not produce a functional TLR2/6 heterodimer complex due to the low level of expression of TLR2 and/or lack a secondary molecule that is required for recognition or a stimulation signal for FSL-1. Future studies will be required to resolve this issue. The lack of TLR4 signaling in our model is not surprising, as it has been shown that HEC-1A cells do not respond to LPS (43), and we have previously shown that epithelial cells lining the lower FRT generally do not respond to LPS (35, 36, 44).

We also examined the expression of mucins, given that the mucus layer that coats the human FRT plays a crucial role in host defense against microbial pathogens. Mucins, which are the major components of mucus, are categorized into two major classes: membrane-associated mucins (MAMs) and secreted gel-forming mucins. These epithelial barrier molecules lubricate mucosal surfaces, play a key role in the innate immune response, and are able to trap pathogens. The full mucin profile of the human endometrium is still not clearly defined due to the complexity of the tissue and menstrual cycle stages. Previous investigators originally showed that MUC1 is expressed in normal endometrial tissue and plays a role in implantation (45, 46). MUC4 expression data differ between laboratories (45, 47, 48) and have yielded conflicting results. MUC2 and MUC16 production in endometrial tissue has been previously reported (48, 49). We showed that the EECs in the 3-D cell culture abundantly express MAMs, including *MUC1*, *MUC4*, *MUC17*, and *MUC20* (Fig. 2). Expression of *MUC1* is consistent with mucin expression in normal endometrial tissue; however, expression of *MUC4*, *MUC17*, and *MUC20* is more typical of cancer tissues. Similar to our findings, Chapela et al. (50) also showed high levels of expression of *MUC4* in the HEC-1A cell line and observed further that *MUC4* expression, as monitored by qRT-PCR, was not affected by sex hormones but was stimulated by proinflammatory cytokines, including TNF-α.

The same study showed that MUC4 can be a potential biomarker for endometrial adenocarcinoma in a subset of patients. Another study demonstrated that MUC4 is the predominant mucin detected in endometrial adenocarcinoma, with 77.1% of samples being positive (48). MUC20 is also overexpressed in ovarian and endometrial cancer tissues (51, 52) and was originally identified in kidney (53). Similarly, MUC17 was shown to be overexpressed in mucinous epithelial ovarian cancer (54). Taken together, all of these observations suggest that the expression of MUC4, MUC17, and MUC20 is related to the tumor origin of the HEC-1A cell line used in this study.

Despite the high levels of expression of cancer-related mucins, our model also produces high levels of the major MAM found in the human endometrium, namely, MUC1 (46). Additionally, the low expression level of secretory mucin MUC5AC in our 3-D EEC model is in accordance with a report showing that MUC5AC is not detectable in the normal endometrial tissues, whereas its levels in pathological tissues are elevated (48). Thus, with respect to mucin expression, our 3-D EEC aggregates appear to have characteristics of both normal and tumor tissue.

In addition to characterizing TLR and mucin expression, we studied host-microbe interactions in this model. For these studies, we selected bacterial species commonly found in the human FRT, including a sexually transmitted pathogen, *N. gonorrhoeae*, and two endogenous vaginal microbes, one of which (*L. crispatus*) is commensal and the other of which (*G. vaginalis*) is associated with BV (18, 19, 33, 55). It should also be noted that both *N. gonorrhoeae* and *G. vaginalis* are associated with endometritis and PID (2, 20, 21, 55, 56). Our results first showed that all tested species are capable of adhering to the 3-D EEC aggregates. In the case of *N. gonorrhoeae*, we observed typically low levels of invasion (0.13%). Second, exposure of our 3-D EEC model to *N. gonorrhoeae* elicited significantly increased levels of expression of all tested proinflammatory immune mediators in a dose-dependent manner (Fig. 5). In contrast, *L. crispatus* and two *G. vaginalis* strains isolated from BV-positive and BV-negative women did not result in a significant induction of proinflammatory cytokines and chemokines (Fig. 5). These results are in accordance with those of a study by Mitchell and colleagues, who observed the presence of vaginal bacterial species in the endometrial cavities of most women undergoing a hysterectomy (18). These investigators also tested endometrial fluid and tissue for cytokines and defensins and showed that colonization of the upper FRT with low levels of vaginal species is not associated with increased levels of inflammatory markers. Furthermore, Schwebke and colleagues (15, 16) hypothesize that *G. vaginalis* initiates the formation of biofilms composed of diverse anaerobic and microaerophilic bacteria. It is possible that *G. vaginalis* individually does not induce an overt proinflammatory response; however, it may require the complex polymicrobial community.

Additionally, in this study we compared a well-characterized *N. gonorrhoeae pilT* deletion mutant, the Δ*pilT* mutant, which produces nonretractible pili, with the wild-type strain. SEM analysis showed differences in the morphology of epithelial cells (i.e., microvillus remodeling) after infection with the wt and the Δ*pilT* mutant strain. These findings are in accordance with previous reports (34, 57). However, this is the first report, to our knowledge, describing gonococcal infection of epithelial cells in a 3-D cell culture. We observed intimate interactions of gonococci with multiple cuboidal cells at their crevices, which could not have been shown using epithelial monolayers (34, 57). Moreover, our SEMs of 3-D EEC aggregates infected with wt *N. gonorrhoeae* and the Δ*pilT* mutant are consistent with reports that *pilT* has a cytoprotective effect on infected cells (34). The wild-type strain also inhibited the secretion of IL-6, whereas the Δ*pilT* mutant showed an impaired ability to induce IL-8 expression through retraction-dependent activation of NF-κB. The cytokine/chemokine profile after infection with both strains was similar to that described previously (58, 59). Those strain-dependent interactions of *N. gonorrhoeae* with epithelial cells show that our 3-D EEC model is a robust tool to study gonorrheal pathogenesis.

Overall, the ability of our model to be colonized with vaginal species, combined with microbe-specific responses that are consistent with clinical findings, demonstrate that

our 3-D EEC model is a robust tool to study host-microbe interactions. Our reductionist approach, outlined in this study, is a foundation for future analyses that could include testing of other individual vaginal species or bacterial mutants. In addition, mixed bacterial cultures, as well as well-characterized clinical samples, could be utilized to model the complex, polymicrobial genital microbiome, including that involved in BV.

In conclusion, our 3-D EEC model recapitulates several key features of *in vivo* endometrial tissue, such as the presence of microvilli and junctional complexes, the production of mucus and secretory material, and a 3-D structure that allows the interaction between microbes and multiple adjacent cells simultaneously. None of these characteristics are exhibited in traditional monolayer cell cultures. The 3-D EEC aggregates also express TLR isoforms and mucins in a pattern that largely mimics that in normal endometrial tissue. These features, including the ability of EEC aggregates to appropriately respond to gonorrheal infection, suggest that our 3-D EEC model is suitable for studying microbial pathogenesis and the host immune response to microbial infection. Together with our well-characterized 3-D vaginal and endocervical epithelial cell models (35, 36), we are now able to study site-specific differences in the biology of the human FRT. In the future, the human 3-D EEC model could be employed to study other STIs, vaginal microbiota, and the effects of exogenous factors to further elucidate the innate immune mechanism at this mucosal site.

MATERIALS AND METHODS

Human endometrial epithelial cell culture. The human endometrial adenocarcinoma cell line HEC-1A was purchased from the American Type Culture Collection (ATTC HTB-112) and cultured in McCoy's 5A medium supplemented with 0.2 mM L-glutamine, 10% heat-inactivated fetal bovine serum, penicillin (100 IU), and streptomycin (100 μg/ml) in a humidified atmosphere of 5% CO_2 at 37°C. For quantification, cells were dissociated with 0.25% (vol/vol) trypsin and counted using trypan blue exclusion staining and a Countess automated cell counter (Invitrogen, Carlsbad, CA). All cell culture media and supplements were purchased from Gibco (Grand Island, NY) or Mediatech (Manassas, VA).

Generation of the human 3-D endometrial epithelial cell model. HEC-1A cells were grown on collagen-coated dextran microcarrier beads (Cytodex-3; Sigma-Aldrich, St. Louis, MO) in a rotating wall vessel (RWV) bioreactor (Synthecon, Houston, TX) to form differentiated 3-D EEC aggregates (22, 25–28, 35, 36). HEC-1A cells were initially grown as monolayers in tissue culture flasks, trypsinized, and counted as described above. Single-cell suspensions (5×10^6 cells) were combined with 250 mg of Cytodex-3 microcarrier beads. The cell-bead suspension was seeded into an RWV bioreactor, and the vessel was filled with cell culture medium and rotated at 20 rpm. The medium was changed at day 4 and daily thereafter. After 21 days in the RWV bioreactor, the 3-D EEC aggregates were fully differentiated, tested for viability as described above, and distributed into 24-well plates (1.4×10^6 to 3.6×10^6 cells/ml) for experimental manipulations.

Mucin production and TLR stimulation. Mucin production was determined by alcian blue staining. Briefly, 3-D EEC aggregates were incubated with 1% (wt/vol) alcian blue 8GX (Sigma-Aldrich) for 30 min at 37°C and then washed with 2.5% (vol/vol) acetic acid and Dulbecco's phosphate-buffered saline (DPBS). Stained mucins were visualized by bright-field microscopy. For testing for Toll-like receptor (TLR) activity, human 3-D EEC aggregates were exposed to the following TLR agonists (InvivoGen, San Diego, CA) for 24 h under standard culturing conditions: fibroblast-stimulating lipoprotein (FSL-1) at 0.1 and 1 μg/ml, FLA-ST (a flagellin purified from *Salmonella enterica* serovar Typhimurium) at 0.5 and 5 μg/ml, LPS-B5 (ultrapure lipopolysaccharide purified from *Escherichia coli* O55:B5) at 1, 0.1, and 0.01 μg/ml, and poly(I·C) at 10 and 100 μg/ml. After treatment, cell culture supernatants and 3-D EEC aggregates were collected from each well and stored at −20°C for further analysis.

Bacterial strains and culture conditions. *L. crispatus* strain VPI-3199 (ATCC 33820) was cultured on lactobacillus MRS agar plates in 5% CO_2 at 37°C. *G. vaginalis* strains JCP8066 (HM-1112) and JCP8161B (HM-1116) were obtained from BEI Resources (NIAID, NIH, as part of the Human Microbiome Project) and cultured on Columbia agar supplemented with 5% defibrinated sheep blood (Quad Five, Ryegate, MT), colistin (10 μg/ml; AdipoGen, San Diego, CA), and nalidixic acid (15 μg/ml; Acros Organics, Geel, Belgium) in 5% CO_2 at 37°C. *Mobiluncus mulieris* strain UPII 28-I (HM-125) was obtained from the BEI Resources collection and cultured on tryptic soy agar supplemented with 5% defibrinated sheep blood (Quad Five) at 37°C under anaerobic conditions, generated with a GasPak EZ anaerobe container system. *N. gonorrhoeae* was grown on GC agar supplemented with 1% (wt/vol) dried bovine hemoglobin and 1% (vol/vol) IsoVitaleX enrichment in 5% CO_2 at 37°C. *N. gonorrhoeae* strain MS11 produces type 4 pilus (Tfp) fibers but does not express *opa* genes (60). The *pilT* open reading frame is deleted in the isogenic Δ*pilT* mutant. It cannot retract Tfp fibers and is deficient in all Tfp retraction-dependent functions (61, 62). All bacterial culture media and supplements were purchased from Becton, Dickinson and Company (Franklin Lakes, NJ) unless otherwise indicated.

Bacterial infection and colonization assays. Bacteria were grown for 18 to 24 h on appropriate agar plates and resuspended in sterile DPBS. Bacteria were quantified by plating serial dilutions of bacterial suspensions. Human 3-D EEC aggregates were seeded in 24-well plates and infected at a

multiplicity of infection (MOI) of 1 to 100 bacteria/cell. Heat-inactivated bacteria were prepared by incubation for 30 min at 55°C. Additional wells were treated with DPBS as a negative control. After incubation for 24 h in 5% CO_2 or under anaerobic conditions at 37°C to allow bacterial colonization, the cell culture supernatants and 3-D EEC aggregates from each well were collected and stored at −20°C for further analysis. Cell cytotoxicity was determined using a Pierce LDH cytotoxicity assay kit (Thermo Scientific, Rockford, IL) in accordance with the manufacturer's protocol. To confirm colonization, infected 3-D EEC aggregates were washed twice with DPBS, and the cells were detached from the microcarrier beads using 1 mM EDTA (Mediatech) or lysed with 0.01% Triton X-100 (Sigma-Aldrich). Cell suspensions were plated on selective media and incubated for 48 to 72 h in 5% CO_2 at 37°C for bacterial quantification.

Electron microscopy. Samples were fixed and processed for transmission electron microscopy (TEM) or scanning electron microscopy (SEM) as described previously (35, 63). Samples processed for TEM were imaged with a transmission electron microscope (model JEM-1200-EX; JEOL, Tokyo, Japan), and images were acquired using a model L3C charge-coupled-device camera (Scientific Instruments and Applications, Duluth, GA). Samples processed for SEM were imaged with a scanning electron microscope (model JSM-6300; JEOL), and images were acquired using an IXRF model 500 digital processor (IXRF Systems Inc., Houston, TX).

RNA purification, reverse transcription-PCR (RT-PCR), and qPCR. RNA was extracted from 3-D EEC aggregates using an RNeasy kit (Qiagen, Valencia, CA) according to the manufacturer's instructions. RNA was quantified using a NanoDrop spectrophotometer (Thermo Scientific). cDNA was generated from 1 μg of total RNA using iScript reverse transcription Supermix for quantitative reverse transcription-PCR (qRT-PCR); (Bio-Rad, Hercules, CA) according to the manufacturer's instructions. Gene expression was measured by qRT-PCR analysis, performed with an Applied Biosystems 7500 Fast real-time PCR system (Life Technologies) using customized primers purchased from Integrated DNA Technologies (Coralville, IA) and iTaq Universal SYBR green Supermix with carboxy-X-rhodamine (Bio-Rad). The following primers were used in this study: chemokine (C-C motif) ligand 20 (CCL20) forward (5′-TTGCTCCTGGCTGCTTTG-3′) and reverse (5′-ACCCTCCATGATGTGCAAG-3′) (64), interleukin 1β (IL-1β) forward (5′-ACAGATGAAGTGC TCCTTCCA-3′) and reverse (5-GTCGGAGATTCGTAGCTGGAT-3′) (65), interleukin 8 (IL-8) forward (5′-ATG ACTTCCAAGCTGGCCGTGGCT-3′) and reverse (5′-TCTCAGCCCTCTTCAAAAACTTCTC-3′) (66), mucin 20 (MUC20) forward (5′-ATCCCGAGGAAGCCATCTTTGACA-3′) and reverse (5′-TTCTGTGGAGGTGTGAGCCAA TGT-3′), and nuclear factor (NF)-κB p105 subunit forward (5′-ACACCGTGTAAACCAAAGCC-3′) and reverse (5′-CAGCCAGTGTTGTGATTGCT-3′). Primers for tumor necrosis factor α (TNF-α), glyceraldehyde 3-phosphate dehydrogenase (GAPDH), mucins, and Toll-like receptors (TLRs) were previously described (36, 44, 67). Relative transcript levels were calculated using the *GAPDH* housekeeping gene transcript level as an internal standard and are reported as the fold change relative to the level for negative treatment controls using the $2^{-\Delta\Delta CT}$ threshold cycle (C_T) method unless otherwise indicated (68).

Chemokine/cytokine quantification. Cell culture supernatants were collected from 3-D EEC aggregates at 24 h postinfection or after exposure to TLR agonists. Secreted chemokines and cytokines were quantified using a Milliplex multianalyte profiling (MAP) human high-sensitivity T cell magnetic bead panel array (Millipore, Billerica, MA) in accordance with the manufacturer's instructions, customized for the following targets: interleukin 6 (IL-6), IL-8, TNF-α, and CCL20. Data were collected with a BioPlex 200 instrument and analyzed using Manager (version 5.0) software (Bio-Rad).

Statistics. All experimental analyses were performed in duplicate using at least three independent batches of 3-D EEC aggregates unless otherwise indicated. An unpaired 2-tailed Student *t* test was performed to determine statistically significance differences between treatment groups. GraphPad Prism (version 5.0) software (GraphPad, San Diego, CA) was used for statistical analysis. *P* values of <0.05 were considered significant.

ACKNOWLEDGMENTS

The following bacterial strains were obtained through BEI Resources, NIAID, NIH, as part of the Human Microbiome Project: *G. vaginalis* strain JCP8066 (HM-1112), *G. vaginalis* strain JCP8151B (HM-1116), and *M. mulieris* strain UPII 28-I (HM-125).

We acknowledge Ryan Smith for cell culture assistance, David Lowry and Robert Roberson from the Arizona State University Electron Microscope Laboratory for technical support, and Graham Kerr Whitfield and Andrea Throop for critical reviews of the manuscript.

This work was supported by the University of Arizona.

M.M.H.-K. contributed to the conception and design of the experiments. P.L., A.G., and G.H. acquired the data. P.L., A.G., G.H., M.S., and M.M.H.-K. all contributed to the analysis and interpretation of the data. P.L., M.S., and M.M.H.-K. drafted the manuscript and revised it critically for intellectual content. All authors approved the final version of the manuscript.

REFERENCES

1. Hillier SL, Nugent RP, Eschenbach DA, Krohn MA, Gibbs RS, Martin DH, Cotch MF, Edelman R, Pastorek JG, II, Rao AV, McNellis D, Regan JA, Carey C, Klebanoff M. 1995. Association between bacterial vaginosis and preterm delivery of a low-birth-weight infant. The Vaginal Infections and Prematurity Study Group. N Engl J Med 333:1737–1742.
2. Taylor BD, Darville T, Haggerty CL. 2013. Does bacterial vaginosis cause

pelvic inflammatory disease? Sex Transm Dis 40:117–122. https://doi.org/10.1097/OLQ.0b013e31827c5a5b.
3. Nelson DB, Bellamy S, Nachamkin I, Ness RB, Macones GA, Allen-Taylor L. 2007. First trimester bacterial vaginosis, individual microorganism levels, and risk of second trimester pregnancy loss among urban women. Fertil Steril 88:1396–1403. https://doi.org/10.1016/j.fertnstert.2007.01.035.
4. Dickson RP, Erb-Downward JR, Martinez FJ, Huffnagle GB. 2016. The microbiome and the respiratory tract. Annu Rev Physiol 78:481–504. https://doi.org/10.1146/annurev-physiol-021115-105238.
5. Brubaker L, Wolfe AJ. 2015. The new world of the urinary microbiota in women. Am J Obstet Gynecol 213:644–649. https://doi.org/10.1016/j.ajog.2015.05.032.
6. Wein AJ. 2015. Re: the microbiome of the urinary tract—a role beyond infection. J Urol 194:1643–1644. https://doi.org/10.1016/j.juro.2015.09.053.
7. Aagaard K, Ma J, Antony KM, Ganu R, Petrosino J, Versalovic J. 2014. The placenta harbors a unique microbiome. Sci Transl Med 6:237ra65. https://doi.org/10.1126/scitranslmed.3008599.
8. Franasiak JM, Werner MD, Juneau CR, Tao X, Landis J, Zhan Y, Treff NR, Scott RT. 2016. Endometrial microbiome at the time of embryo transfer: next-generation sequencing of the 16S ribosomal subunit. J Assist Reprod Genet 33:129–136. https://doi.org/10.1007/s10815-015-0614-z.
9. Verstraelen H, Vilchez-Vargas R, Desimpel F, Jauregui R, Vankeirsbilck N, Weyers S, Verhelst R, De Sutter P, Pieper DH, Van De Wiele T. 2016. Characterisation of the human uterine microbiome in non-pregnant women through deep sequencing of the V1-2 region of the 16S rRNA gene. PeerJ Preprints 4:e1602. https://doi.org/10.7717/peerj.1602.
10. Ulcova-Gallova Z. 2010. Immunological and physicochemical properties of cervical ovulatory mucus. J Reprod Immunol 86:115–121. https://doi.org/10.1016/j.jri.2010.07.002.
11. Yarbrough VL, Winkle S, Herbst-Kralovetz MM. 2015. Antimicrobial peptides in the female reproductive tract: a critical component of the mucosal immune barrier with physiological and clinical implications. Hum Reprod Update 21:353–377. https://doi.org/10.1093/humupd/dmu065.
12. Becher N, Hein M, Danielsen CC, Uldbjerg N. 2010. Matrix metalloproteinases in the cervical mucus plug in relation to gestational age, plug compartment, and preterm labor. Reprod Biol Endocrinol 8:113. https://doi.org/10.1186/1477-7827-8-113.
13. Hansen LK, Becher N, Bastholm S, Glavind J, Ramsing M, Kim CJ, Romero R, Jensen JS, Uldbjerg N. 2014. The cervical mucus plug inhibits, but does not block, the passage of ascending bacteria from the vagina during pregnancy. Acta Obstet Gynecol Scand 93:102–108. https://doi.org/10.1111/aogs.12296.
14. Fredricks DN, Fiedler TL, Marrazzo JM. 2005. Molecular identification of bacteria associated with bacterial vaginosis. N Engl J Med 353:1899–1911. https://doi.org/10.1056/NEJMoa043802.
15. Muzny CA, Schwebke JR. 2016. Pathogenesis of bacterial vaginosis: discussion of current hypotheses. J Infect Dis 214(Suppl 1):S1–S5. https://doi.org/10.1093/infdis/jiw121.
16. Schwebke JR, Muzny CA, Josey WE. 2014. Role of Gardnerella vaginalis in the pathogenesis of bacterial vaginosis: a conceptual model. J Infect Dis 210:338–343. https://doi.org/10.1093/infdis/jiu089.
17. Bradshaw CS, Sobel JD. 2016. Current treatment of bacterial vaginosis—limitations and need for innovation. J Infect Dis 214(Suppl 1):S14–S20. https://doi.org/10.1093/infdis/jiw159.
18. Mitchell CM, Haick A, Nkwopara E, Garcia R, Rendi M, Agnew K, Fredricks DN, Eschenbach D. 2015. Colonization of the upper genital tract by vaginal bacterial species in nonpregnant women. Am J Obstet Gynecol 212:611.e1–e9. https://doi.org/10.1016/j.ajog.2014.11.043.
19. Swidsinski A, Verstraelen H, Loening-Baucke V, Swidsinski S, Mendling W, Halwani Z. 2013. Presence of a polymicrobial endometrial biofilm in patients with bacterial vaginosis. PLoS One 8:e53997. https://doi.org/10.1371/journal.pone.0053997.
20. Reighard SD, Sweet RL, Vicetti Miguel C, Vicetti Miguel RD, Chivukula M, Krishnamurti U, Cherpes TL. 2011. Endometrial leukocyte subpopulations associated with Chlamydia trachomatis, Neisseria gonorrhoeae, and Trichomonas vaginalis genital tract infection. Am J Obstet Gynecol 205:324.e1–e7. https://doi.org/10.1016/j.ajog.2011.05.031.
21. Wiesenfeld HC, Hillier SL, Krohn MA, Amortegui AJ, Heine RP, Landers DV, Sweet RL. 2002. Lower genital tract infection and endometritis: insight into subclinical pelvic inflammatory disease. Obstet Gynecol 100:456–463.
22. Goodwin TJ, Schroeder WF, Wolf DA, Moyer MP. 1993. Rotating-wall vessel coculture of small intestine as a prelude to tissue modeling: aspects of simulated microgravity. Proc Soc Exp Biol Med 202:181–192. https://doi.org/10.3181/00379727-202-43525.
23. Barrila J, Radtke AL, Crabbe A, Sarker SF, Herbst-Kralovetz MM, Ott CM, Nickerson CA. 2010. Organotypic 3D cell culture models: using the rotating wall vessel to study host-pathogen interactions. Nat Rev Microbiol 8:791–801. https://doi.org/10.1038/nrmicro2423.
24. Herbst-Kralovetz MM, Pyles RB, Ratner AJ, Sycuro LK, Mitchell C. 2016. New systems for studying intercellular interactions in bacterial vaginosis. J Infect Dis 214:S6–S13. https://doi.org/10.1093/infdis/jiw130.
25. Griffith LG, Swartz MA. 2006. Capturing complex 3D tissue physiology in vitro. Nat Rev Mol Cell Biol 7:211–224. https://doi.org/10.1038/nrm1858.
26. Schmeichel KL, Bissell MJ. 2003. Modeling tissue-specific signaling and organ function in three dimensions. J Cell Sci 116:2377–2388. https://doi.org/10.1242/jcs.00503.
27. Ingber DE. 2008. Tensegrity-based mechanosensing from macro to micro. Prog Biophys Mol Biol 97:163–179. https://doi.org/10.1016/j.pbiomolbio.2008.02.005.
28. Radtke AL, Herbst-Kralovetz MM. 2012. Culturing and applications of rotating wall vessel bioreactor derived 3D epithelial cell models. J Vis Exp 2012:3868. https://doi.org/10.3791/3868.
29. Kuramoto H, Tamura S, Notake Y. 1972. Establishment of a cell line of human endometrial adenocarcinoma in vitro. Am J Obstet Gynecol 114:1012–1019. https://doi.org/10.1016/0002-9378(72)90861-7.
30. Ludwig H, Metzger H. 1979. Human female reproductive tract: a scanning electron microscopy atlas. Springer-Verlag, New York, NY.
31. Aflatoonian R, Tuckerman E, Elliott SL, Bruce C, Aflatoonian A, Li TC, Fazeli A. 2007. Menstrual cycle-dependent changes of Toll-like receptors in endometrium. Hum Reprod 22:586–593. https://doi.org/10.1093/humrep/del388.
32. Schaefer TM, Desouza K, Fahey JV, Beagley KW, Wira CR. 2004. Toll-like receptor (TLR) expression and TLR-mediated cytokine/chemokine production by human uterine epithelial cells. Immunology 112:428–436. https://doi.org/10.1111/j.1365-2567.2004.01898.x.
33. Sharma H, Tal R, Clark NA, Segars JH. 2014. Microbiota and pelvic inflammatory disease. Semin Reprod Med 32:43–49. https://doi.org/10.1055/s-0033-1361822.
34. Higashi DL, Lee SW, Snyder A, Weyand NJ, Bakke A, So M. 2007. Dynamics of Neisseria gonorrhoeae attachment: microcolony development, cortical plaque formation, and cytoprotection. Infect Immun 75:4743–4753. https://doi.org/10.1128/IAI.00687-07.
35. Hjelm BE, Berta AN, Nickerson CA, Arntzen CJ, Herbst-Kralovetz MM. 2010. Development and characterization of a three-dimensional organotypic human vaginal epithelial cell model. Biol Reprod 82:617–627. https://doi.org/10.1095/biolreprod.109.080408.
36. Radtke AL, Quayle AJ, Herbst-Kralovetz MM. 2012. Microbial products alter the expression of membrane-associated mucin and antimicrobial peptides in a three-dimensional human endocervical epithelial cell model. Biol Reprod 87:132. https://doi.org/10.1095/biolreprod.112.103366.
37. Illouz S, Dales JP, Sferlazzo K, Garcia S, Carpentier-Meunier S, Boubli L, Lavaut MN, Charpin C. 2003. Effects of progestins of human proliferative endometrium: an in vitro model of potential clinical relevance. Int J Mol Med 12:517–523. https://doi.org/10.3892/ijmm.12.4.517.
38. Sharma M, Shubert DE, Sharma M, Rodabaugh KJ, McGarrigle BP, Vezina CM, Bofinger DP, Olson JR. 2003. Antioxidant inhibits tamoxifen-DNA adducts in endometrial explant culture. Biochem Biophys Res Commun 307:157–164. https://doi.org/10.1016/S0006-291X(03)01134-3.
39. Sharma M, Shubert DE, Sharma M, Lewis J, McGarrigle BP, Bofinger DP, Olson JR. 2003. Biotransformation of tamoxifen in a human endometrial explant culture model. Chem Biol Interact 146:237–249. https://doi.org/10.1016/j.cbi.2003.06.002.
40. Blauer M, Heinonen PK, Martikainen PM, Tomas E, Ylikomi T. 2005. A novel organotypic culture model for normal human endometrium: regulation of epithelial cell proliferation by estradiol and medroxyprogesterone acetate. Hum Reprod 20:864–871. https://doi.org/10.1093/humrep/deh722.
41. Korch C, Spillman MA, Jackson TA, Jacobsen BM, Murphy SK, Lessey BA, Jordan VC, Bradford AP. 2012. DNA profiling analysis of endometrial and ovarian cell lines reveals misidentification, redundancy and contamination. Gynecol Oncol 127:241–248. https://doi.org/10.1016/j.ygyno.2012.06.017.
42. Fazeli A, Bruce C, Anumba DO. 2005. Characterization of Toll-like recep-

tors in the female reproductive tract in humans. Hum Reprod 20:1372–1378. https://doi.org/10.1093/humrep/deh775.
43. Cremel M, Hamzeh-Cognasse H, Genin C, Delezay O. 2006. Female genital tract immunization: evaluation of candidate immunoadjuvants on epithelial cell secretion of CCL20 and dendritic/Langerhans cell maturation. Vaccine 24:5744–5754. https://doi.org/10.1016/j.vaccine.2006.04.044.
44. Herbst-Kralovetz MM, Quayle AJ, Ficarra M, Greene S, Rose WA, II, Chesson R, Spagnuolo RA, Pyles RB. 2008. Quantification and comparison of Toll-like receptor expression and responsiveness in primary and immortalized human female lower genital tract epithelia. Am J Reprod Immunol 59:212–224. https://doi.org/10.1111/j.1600-0897.2007.00566.x.
45. Gipson IK, Ho SB, Spurr-Michaud SJ, Tisdale AS, Zhan Q, Torlakovic E, Pudney J, Anderson DJ, Toribara NW, Hill JA, III. 1997. Mucin genes expressed by human female reproductive tract epithelia. Biol Reprod 56:999–1011. https://doi.org/10.1095/biolreprod56.4.999.
46. Constantinou PE, Morgado M, Carson DD. 2015. Transmembrane mucin expression and function in embryo implantation and placentation. Adv Anat Embryol Cell Biol 216:51–68. https://doi.org/10.1007/978-3-319-15856-3_4.
47. Koscinski I, Viville S, Porchet N, Bernigaud A, Escande F, Defossez A, Buisine MP. 2006. MUC4 gene polymorphism and expression in women with implantation failure. Hum Reprod 21:2238–2245. https://doi.org/10.1093/humrep/del189.
48. Alameda F, Mejias-Luque R, Garrido M, de Bolos C. 2007. Mucin genes (MUC2, MUC4, MUC5AC, and MUC6) detection in normal and pathological endometrial tissues. Int J Gynecol Pathol 26:61–65. https://doi.org/10.1097/01.pgp.0000225837.32719.c1.
49. Dharmaraj N, Chapela PJ, Morgado M, Hawkins SM, Lessey BA, Young SL, Carson DD. 2014. Expression of the transmembrane mucins, MUC1, MUC4 and MUC16, in normal endometrium and in endometriosis. Hum Reprod 29:1730–1738. https://doi.org/10.1093/humrep/deu146.
50. Chapela PJ, Broaddus RR, Hawkins SM, Lessey BA, Carson DD. 2015. Cytokine stimulation of MUC4 expression in human female reproductive tissue carcinoma cell lines and endometrial cancer. J Cell Biochem 116:2649–2657. https://doi.org/10.1002/jcb.25213.
51. Chen CH, Wang SW, Chen CW, Huang MR, Hung JS, Huang HC, Lin HH, Chen RJ, Shyu MK, Huang MC. 2013. MUC20 overexpression predicts poor prognosis and enhances EGF-induced malignant phenotypes via activation of the EGFR-STAT3 pathway in endometrial cancer. Gynecol Oncol 128:560–567. https://doi.org/10.1016/j.ygyno.2012.12.012.
52. Chen CH, Shyu MK, Wang SW, Chou CH, Huang MJ, Lin TC, Chen ST, Lin HH, Huang MC. 2016. MUC20 promotes aggressive phenotypes of epithelial ovarian cancer cells via activation of the integrin beta1 pathway. Gynecol Oncol 140:131–137. https://doi.org/10.1016/j.ygyno.2015.11.025.
53. Higuchi T, Orita T, Nakanishi S, Katsuya K, Watanabe H, Yamasaki Y, Waga I, Nanayama T, Yamamoto Y, Munger W, Sun HW, Falk RJ, Jennette JC, Alcorta DA, Li H, Yamamoto T, Saito Y, Nakamura M. 2004. Molecular cloning, genomic structure, and expression analysis of MUC20, a novel mucin protein, up-regulated in injured kidney. J Biol Chem 279:1968–1979. https://doi.org/10.1074/jbc.M304558200.
54. Heinzelmann-Schwarz VA, Gardiner-Garden M, Henshall SM, Scurry JP, Scolyer RA, Smith AN, Bali A, Vanden Bergh P, Baron-Hay S, Scott C, Fink D, Hacker NF, Sutherland RL, O'Brien PM. 2006. A distinct molecular profile associated with mucinous epithelial ovarian cancer. Br J Cancer 94:904–913. https://doi.org/10.1038/sj.bjc.6603003.
55. Haggerty CL, Totten PA, Tang G, Astete SG, Ferris MJ, Norori J, Bass DC, Martin DH, Taylor BD, Ness RB. 2016. Identification of novel microbes associated with pelvic inflammatory disease and infertility. Sex Transm Infect 92:441–446. https://doi.org/10.1136/sextrans-2015-052285.
56. Haggerty CL, Hillier SL, Bass DC, Ness RB, PID Evaluation and Clinical Health Study Investigators. 2004. Bacterial vaginosis and anaerobic bacteria are associated with endometritis. Clin Infect Dis 39:990–995. https://doi.org/10.1086/423963.
57. Griffiss JM, Lammel CJ, Wang J, Dekker NP, Brooks GF. 1999. Neisseria gonorrhoeae coordinately uses pili and Opa to activate HEC-1-B cell microvilli, which causes engulfment of the gonococci. Infect Immun 67:3469–3480.
58. Dietrich M, Bartfeld S, Munke R, Lange C, Ogilvie LA, Friedrich A, Meyer TF. 2011. Activation of NF-kappaB by Neisseria gonorrhoeae is associated with microcolony formation and type IV pilus retraction. Cell Microbiol 13:1168–1182. https://doi.org/10.1111/j.1462-5822.2011.01607.x.
59. Calton CM, Wade LK, So M. 2013. Upregulation of ATF3 inhibits expression of the pro-inflammatory cytokine IL-6 during Neisseria gonorrhoeae infection. Cell Microbiol 15:1837–1850. https://doi.org/10.1111/cmi.12153.
60. Segal E, Hagblom P, Seifert HS, So M. 1986. Antigenic variation of gonococcal pilus involves assembly of separated silent gene segments. Proc Natl Acad Sci U S A 83:2177–2181. https://doi.org/10.1073/pnas.83.7.2177.
61. Merz AJ, So M, Sheetz MP. 2000. Pilus retraction powers bacterial twitching motility. Nature 407:98–102. https://doi.org/10.1038/35024105.
62. Wolfgang M, Lauer P, Park HS, Brossay L, Hebert J, Koomey M. 1998. PilT mutations lead to simultaneous defects in competence for natural transformation and twitching motility in piliated Neisseria gonorrhoeae. Mol Microbiol 29:321–330. https://doi.org/10.1046/j.1365-2958.1998.00935.x.
63. McGowin CL, Radtke AL, Abraham K, Martin DH, Herbst-Kralovetz M. 2013. Mycoplasma genitalium infection activates cellular host defense and inflammation pathways in a 3-dimensional human endocervical epithelial cell model. J Infect Dis 207:1857–1868. https://doi.org/10.1093/infdis/jit101.
64. Dieu MC, Vanbervliet B, Vicari A, Bridon JM, Oldham E, Ait-Yahia S, Briere F, Zlotnik A, Lebecque S, Caux C. 1998. Selective recruitment of immature and mature dendritic cells by distinct chemokines expressed in different anatomic sites. J Exp Med 188:373–386. https://doi.org/10.1084/jem.188.2.373.
65. Stordeur P, Poulin LF, Craciun L, Zhou L, Schandene L, de Lavareille A, Goriely S, Goldman M. 2002. Cytokine mRNA quantification by real-time PCR. J Immunol Methods 259:55–64. https://doi.org/10.1016/S0022-1759(01)00489-6.
66. Zhong WW, Burke PA, Hand AT, Walsh MJ, Hughes LA, Forse RA. 1993. Regulation of cytokine mRNA expression in lipopolysaccharide-stimulated human macrophages. Arch Surg 128:158–164. https://doi.org/10.1001/archsurg.1993.01420140035006.
67. Doerflinger SY, Throop AL, Herbst-Kralovetz MM. 2014. Bacteria in the vaginal microbiome alter the innate immune response and barrier properties of the human vaginal epithelia in a species-specific manner. J Infect Dis 209:1989–1999. https://doi.org/10.1093/infdis/jiu004.
68. Schmittgen TD, Livak KJ. 2008. Analyzing real-time PCR data by the comparative C(T) method. Nat Protoc 3:1101–1108. https://doi.org/10.1038/nprot.2008.73.
69. Wang H, Pilla F, Anderson S, Martinez-Escribano S, Herrer I, Moreno-Moya JM, Musti S, Bocca S, Oehninger S, Horcajadas JA. 2012. A novel model of human implantation: 3D endometrium-like culture system to study attachment of human trophoblast (Jar) cell spheroids. Mol Hum Reprod 18:33–43. https://doi.org/10.1093/molehr/gar064.